

LiCamGait: Gait Recognition in the Wild by Using LiDAR and Camera Multi-modal Visual Sensors

Xiao Han Peishan Cong Lan Xu Jingya Wang Jingyi Yu Yuexin Ma
ShanghaiTech University

{hanxiao2022,mayuexin}@shanghaitech.edu.cn

Abstract

LiDAR can capture accurate depth information in large-scale scenarios without the effect of light conditions, and the captured point cloud contains gait-related 3D geometric properties and dynamic motion characteristics. We make the first attempt to leverage LiDAR to remedy the limitation of view-dependent and light-sensitive camera for more robust and accurate gait recognition. In this paper, we propose a LiDAR-camera-based gait recognition method with an effective multi-modal feature fusion strategy, which fully exploits advantages of both point clouds and images. In particular, we propose a new in-the-wild gait dataset, LiCamGait, involving multi-modal visual data and diverse 2D/3D representations. Our method achieves state-of-the-art performance on the new dataset. **Code and dataset will be released when this paper is published.**

1. Introduction

Gait is a promising biometric feature for human identification, which is hard to disguise and can be easily captured at a long distance without any intrusive interactions with subjects. To explore its huge potential in social security, the gait recognition task by identifying a person from sequences of visual data, has been studied for decades [23, 36, 47].

The mainstream methods are based on the camera sensor to capture walking videos of subjects. They process images to silhouettes [7, 13, 17, 30] for gait feature extraction to avoid the interference of color and texture. However, the body shape in silhouette is also affected by changing clothes or carrying bags, causing the network still tends to learn the appearance feature rather than the gait feature. To further eliminate the effect of decorations, some works [37, 46] exploit the skeletons for gait recognition. However, the skeleton generated from image also relies on the image quality. All above methods suffer from the view-dependent property of images and the lack of depth information, which results in the ambiguity of gait characteristics. As Figure 1 shows,

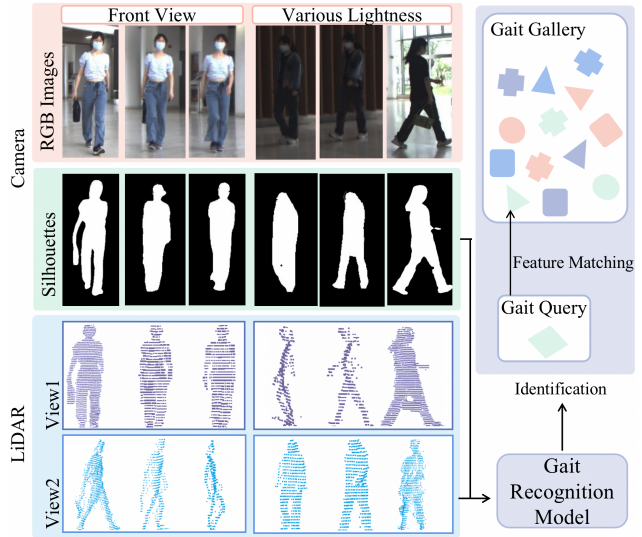


Figure 1. Images always bring the ambiguity of gait characteristics due to the view-dependent property and the lack of depth information. Meanwhile, camera is sensitive to light, resulting in unstable performance with changing illumination. LiDAR can work day and night and capture view-independent depth information, which is friendly for extracting geometry and dynamic features of gait. A novel LiDAR-camera multi-sensor setting is proposed for robust gait recognition in the wild.

it is difficult to distinguish gait-related properties in front-view images, such as stride size and frequency. Moreover, camera is light-sensitive and the low-quality images captured in poor light conditions will lead to terrible silhouette or skeleton results, which will further affect the identification accuracy. Although recent work [60] tries to alleviate the problem by taking 3D parametric model of human body estimated from image as auxiliary input, it still could not escape from camera limitations and has accumulative errors.

Compared with camera, LiDAR can capture accurate depth information in large-scale indoor and outdoor scenes and is not affected by illumination conditions, which has already been widely used in autonomous driving [18, 62] and robotics. And some recent works [10, 11, 24, 59] begin to

explore the potential of LiDAR in human-centric perception and motion capture tasks. Actually, LiDAR point cloud of subjects contains real gait-related geometry features and dynamic motion features. Such 3D information is independent of changing views, which can definitely benefit gait recognition, as Figure 1 shows.

Considering the dense representation of image can facilitate the network to extract structural feature of human body, which are what sparse and unordered LiDAR point cloud lacks, we propose a novel gait recognition solution by leveraging both LiDAR and camera sensors. However, due to the huge domain gap between image and point cloud data representations, it is challenging to fuse two-modal visual features reasonably. Previous feature-fusion approaches [5, 28, 50, 51] are designed for perception tasks in traffic scenarios, which are limited for gait recognition task, which requires fine-grained features from local and global human body. Especially, we propose an effective Geometry-Dynamic-Aware (GDA) sensor-fusion strategy by making the network automatically match corresponding point cloud features to each location on the silhouette feature map without any calibration priors. By cross attention mechanism, valuable geometry and dynamic features of point cloud are selected to enhance the dense 2D features. And then, we adopt the commonly-used horizontal pyramid mapping technique for the final human identification.

In particular, to facilitate the research of multi-modal gait recognition, we collect a new dataset, named LiCamGait, by synchronized LiDAR and camera in the wild. Apart from 2D silhouettes and 3D point clouds, our dataset also provides diverse representations, including 2D/3D pose and 3D Mesh & SMPL, in order to promote further research.

Extensive experiments show that our method achieves state-of-the-art performance on LiCamGait and we also provide sufficient analysis on the potential of LiDAR-camera setting. Main contributions can be summarized as below.

- We are the first to explore LiDAR-camera-based gait recognition in free environment, which is insensitive to light changing, view changing, and indoor or outdoor scenarios.
- We propose a novel gait recognition method based on multi-modal visual data. Especially, an effective feature-fusion strategy is designed for fully using the dense representation of images and the geometry and dynamic information in point cloud.
- We propose a new gait recognition dataset, LiCamGait, which contains both 2D silhouettes and 3D point clouds collected in the wild.
- Our method achieves SOTA performance on LiCamGait. And we also provide extensive exploration and analysis on the potential of LiDAR-camera setting.

2. Related Work

2.1. Gait Recognition Methods

Previous gait recognition methods [23, 47] are mainly based on 2D image representation and can be divided into appearance-based and model-based approaches. The former [7, 13, 17, 19, 30] utilizes silhouettes processed from RGB images as input, causing the performance to rely heavily on the quality of segmentation in the pre-processing. Moreover, the features extracted from silhouettes are highly correlated with the capture view and the appearance of subjects at present, which leads the network difficult to identify human with changed clothes or from various views. Model-based methods [3, 4, 12, 21, 25, 29, 37, 46, 55] try to obtain the real gait-related features by taking skeletons as input, which are usually manually annotated or estimated through pose estimation methods from RGB images. However, such methods are limited to predefined structural human body model and still suffer from the view-dependent image representation.

To alleviate the view constraint and depth ambiguity in 2D silhouettes, some gait recognition methods [1, 60] based on 3D representation of humans are proposed in recent years. Gait3D [60] makes the fusion of silhouettes and 3D SMPL [31] models to solve the appearance ambiguity of images. However, the 3D meshes are generated from 2D RGB images, which are still sensitive to the image quality and bring cumulative error for human identification. Some works [1, 6] explore view-robust gait recognition frameworks based on LiDAR point cloud. However, they all project 3D point cloud into image representation for feature extraction, which loses the original 3D geometry information and gets limited performance. Considering that 2D Silhouette provides dense body structure features and 3D point cloud can reflect human’s real geometry information and gait-related physical attributes, like stride length and frequency, we propose a LiDAR-camera multi-sensor-based gait recognition method, which can solve the above limitations.

2.2. Gait Recognition Dataset

Current available gait datasets [20, 33, 45, 53, 57, 63] are mainly silhouette-based. CASIA-series [45, 53, 57] make the first exploration on images for gait recognition and OUISIR [20, 33] series further enlarge the dataset scale with more complex variants, including different combinations of clothing [16], carrying [48], speeds [33], and views [34]. However, the above two series of gait datasets are limited to in-the-lab environments, which is not suitable for real-world applications in the wild. Then, GREW [63] collects a dataset in an open area. To solve the distortion problem existing in view-dependent images, Gait3D [60] provides extra 3D mesh and SMPL generated from RGB im-

ages by ROMP [43] to enrich the input information. However, the auxiliary 3D information is still obtained from 2D images and cannot represent the real depth and 3D dynamic motion properties. LGA [6] collects a gait dataset by LiDAR sensor, which can capture accurate depth information in large-scale scenes, but it only involves 28 subjects and very limited sequences, which is not enough for evaluating learning-based approaches. To facilitate the community of gait recognition, we make the first attempt toward LiDAR-camera-based 3D gait recognition in free environments and collect the first gait recognition dataset containing multi-modal visual data.

2.3. LiDAR-based Applications

LiDAR can capture accurate depth information for large-scale scenarios and is not affected by light conditions, which has been widely used in autonomous driving and robotics. Many LiDAR-based detection [8, 10, 39, 42, 56, 61] and segmentation [2, 35, 54, 58, 62] methods appear and occupy an important place in the field of 3D perception. Afterwards, many human-related applications take LiDAR into consideration to enlarge the usage scenarios and to improve the performance by utilizing the location and geometry feature existing in LiDAR point cloud. LiDARCap [24] and LIP [59] propose the LiDAR-only and LiDAR-camera-based 3D human motion capture methods. HSC4D [11] designs an online scene capture method in large-scale indoor-outdoor space using wearable IMUs and LiDAR. Inspired by the above human-related applications based on LiDAR, we propose a novel benchmark for gait recognition with the aid of LiDAR and camera for human identification to benefit the field of intelligent surveillance and social security.

2.4. LiDAR-Camera Fusion Methods

To take full advantage of both LiDAR and camera, many researchers focus on exploring effective multi-modal feature-fusion methods for more accurate perception. Point cloud features are enriched in PointPainting [50] and PointAugmentation [51] by appended with the local RGB or image features from the projected image position, while such point-level methods suffer from the sparsity of LiDAR point cloud. They are not suitable for the gait recognition task due to the neglect of dense features on silhouettes. Some feature-level fusion methods [9, 22, 27, 38] directly concatenate or multiply multi-modal features, while these methods overlook local feature correspondences between two modalities. [5, 26, 28] utilize transformer strategy for fusing two modalities in voxel or BEV space, which adaptively capture the correlations between image and LiDAR features. However, they target for perception tasks of autonomous driving in large traffic scenarios but are limited to gait recognition, which concerns more fine-grained features. We propose an effective sensor-fusion method for

Table 1. Comparison of public datasets for gait recognition. Cam means camera, Silh. is silhouette, and Free Env. denotes free environment.

Dataset	Sensor	Data Type	Free Env.
CASIA-A [53]	Cam	RGB, Silh.	no
USF HumanID [41]	Cam	RGB	no
CASIA-B [57]	Cam	RGB, Silh.	no
CASIA-C [45]	Cam	Infrared, Silh.	no
OU-ISIR Speed [33]	Cam	Silh.	no
OU-ISIR-LP [20]	Cam	Silh.	no
OU-MVLP [44]	Cam	Silh.	no
OU-MVLP Pose [4]	Cam	2D pose	no
GREW [63]	Cam	Silh., 2D/3D Pose, Flow	Yes
Gait3D [60]	Cam	Silh., 2D/3D Pose, 3D Mesh&SMPL	Yes
LGA [6]	LiDAR	Point Cloud	Yes
LiCamGait	LiDAR & Cam	Silh., Point Cloud, 2D/3D Pose, 3D Mesh&SMPL	Yes

gait recognition by making the network automatically fuse valuable point cloud features to dense image features.

3. Dataset

3.1. Overview of LiCamGait

LiCamGait is the first multi-sensor captured gait recognition dataset. It is collected in the wild with a monocular camera and a 128-beam OuSTER-1 LiDAR, which are mounted together and synchronized at 10fps. The dataset consists of 103 subjects with 63 males and 40 females. All subjects walk freely without any predefined path. We randomly select 71 subjects as the training set and 32 subjects as the testing set. LiCamGait has 4251 sequences in total, where each sequence contains continuously paired silhouettes and LiDAR point clouds with 30 frames on average.

LiDAR can serve long-range perception for autonomous vehicles day and night in large-scale traffic scenarios with the radius of about 50m. However, human is much smaller than common vehicles, making the valid perception range for identifiable human body is about 20m. For the LiDAR configuration we use, the number of points for the subject 20m far from the sensor is about 50. In addition, it is difficult to accurately detect the subject in images when the distance is more than 15m. Therefore, we collect the data mainly in the range of 2m-15m from sensors to ensure the quality of images and point clouds. Actually, the range is still much longer than existing gait datasets.

Compared with previous gait datasets, LiCamGait is special for its diverse visual modalities, rich data representations, free-environment collection, and abundant trajectories and decorations of subjects. Details are shown in Table 1 and Figure 2. More analyses are in the following.

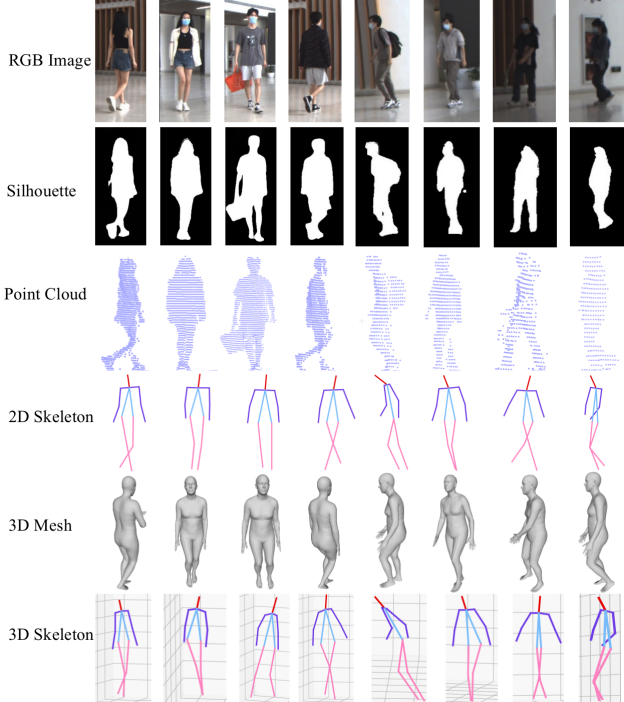


Figure 2. Examples in various light conditions and distances of LiCamGait with multiple modalities and 2D/3D representations.

3.2. Characteristics of LiCamGait

Diverse Visual Modalities. The image captured by camera in regular and dense representation is easy for feature extraction by neural networks. However, the view-dependent property leads to geometry feature ambiguity and motion information inaccuracy. The point cloud captured by LiDAR contains accurate depth and rich geometry information, which can better reflect real gait-related attributes, such as stride size and frequency. All existing gait datasets [1, 20, 57, 63] provide single modal visual data or extra auxiliary representation [60] obtained images. LiCamGait provides multi-modal visual data, including 2D silhouettes and 3D point clouds, which is significant for the exploration of novel sensor settings for gait recognition in the wild.

Diverse Representations. We use current state-of-the-art segmentation methods fine-tuned on our dataset to get 2D silhouettes and 3D point clouds for individuals, including HRNet-segmentation [52] and DSNet [15]. We further provide diverse representations, comprised of 2D/3D pose and 3D Mesh & SMPL, as Figure 2 shows. 2D keypoints of the person in each frame are estimated from HRNet [52]. For the 3D SMPL, 3D mesh, and 3D pose, they can be efficiently extracted from current method [43], similar to [60]. The shape and pose of human body in the 3D space can provide gait-related and appearance-unrelated information, which are crucial for learning discriminative gait features

for human identification. Various representations in LiCamGait can definitely benefit future research.

Free Environment. LiDAR can collect data in fully-unconstrained environments, no matter indoor or outdoor scenes. Especially, in outdoor scenarios, camera is a light-sensitive sensor and the image segmentation quality always suffers from poor light conditions. While LiDAR is not affected by illumination and can work day and night. The background in LiCamGait is complex with various light and weather conditions, which is significant for evaluating the robustness of algorithms for real applications.

Free Trajectories and Decorations. We collect free trajectories of subjects and provide diverse views of visual data in the query sequences. It is important to evaluate the generalization capability of algorithms for view-changing situations. Besides, subjects have multiple choices for decorations, such as wearing different coats or carrying disparate bags. We further divide our dataset into **Norm, Bag, Coat** three subsets according to the decoration categories, which can better verify the robustness of methods under appearance-changing conditions.

3.3. Privacy Preservation

We strictly obey the privacy-preserving rules. We will not release any original RGB images. The silhouettes and LiDAR point clouds without any texture and face information can naturally protect the human privacy.

4. Methodology

4.1. Overview

We propose a novel LiDAR-camera-based gait recognition solution with an effective multi-modality fusion strategy. The overview of our pipeline is shown in Figure 3. We take consecutive 2D silhouettes and 3D point clouds as input and aim to identify individuals based on the way they walk. There are three main procedures in our network, including feature extraction for each kind of visual data, multi-modal feature fusion, and horizontal pyramid matching for person identification. First, convolutional neural network (CNN) and multi-layer perceptron (MPL) are used to extract valuable features from silhouettes and point clouds, respectively. In particular, to combine the dense appearance feature of silhouettes with the geometry and dynamic motion information in point clouds, we propose a novel fusion method named Geometry-Dynamic-Aware Feature Fusion (GDA), which utilizes transformer to make the network automatically finds the corresponding relation between image and point cloud and grasp valuable gait-related feature from point cloud to enhance the silhouette feature. Then, the popular horizontal pyramid matching (HPM) is adopted to gather local and global spatial features and temporal features for making the final prediction. Next, We introduce

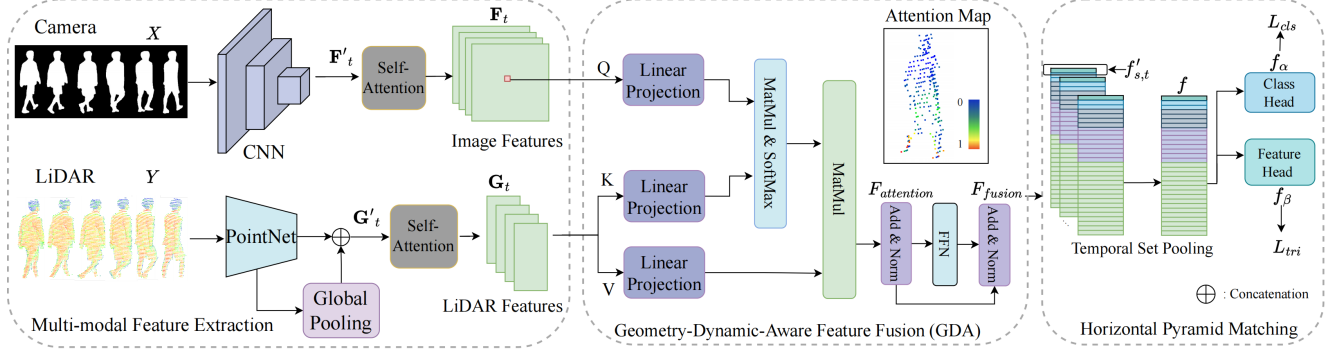


Figure 3. The pipeline of our method. For the input sequence of silhouettes and point clouds, we extract features for each modality first. Then, the geometry-dynamic-aware feature fusion module is applied to fuse two-modal visual features effectively to make use of advantages of both LiDAR and camera sensors. Finally, the following HPM aggregates structural features for the identification.

details of each module of our method.

4.2. Multi-modal Feature Extraction

For the camera branch, we take a sequence with fixed frames of silhouettes $X = \{\mathbf{x}_t\}_{t=1}^T$ as input, where $\mathbf{x}_t \in \mathbb{R}^{H \times W}$ is the t_{th} frame, T is the length of the sequence, H and W are the height and width of the silhouette image, respectively. The image features $\mathbf{F}'_t \in \mathbb{R}^{H \times W}$ for each frame is extracted from 2D CNN backbone with four convolutions layers: $\mathbf{F}'_t = \text{CNN}(x_t)$. Then, we flatten 2D features to one dimension and concatenate them along the temporal dimension.

For the LiDAR branch, the original consecutive frames of point cloud $Y = \{\mathbf{y}_t\}_{t=1}^T$ are fed into a PointNet [40] encoder to obtain continuous geometry feature for each point. $\mathbf{y}_t \in \mathbb{R}^{N \times 4}$ includes x , y , z coordinates and reflectivity, where N stands for the number of points. A global pooling \mathcal{G} is applied to get the high-dimensional semantic feature, which is concatenated with the original local geometry feature to get the point cloud feature $\mathbf{G}'_t \in \mathbb{R}^n$:

$$\mathbf{G}'_t = \mathcal{G}(\text{PointNet}(y_t)) \oplus \text{PointNet}(y_t). \quad (1)$$

To encode more global context information, we use a self-attention [49] block to enhance the spatial feature for each modality and acquire the final silhouette feature \mathbf{F}_t and point cloud feature \mathbf{G}_t for each frame.

4.3. Geometry-Dynamic-Aware Feature Fusion

It is difficult to capture real dynamic gait characteristics from silhouettes due to the depth ambiguity and distorted body shapes in different views. LiDAR point cloud represents the real depth and contains relative location information, which can reflect the geometric properties of a subject body, such as the height, and can provide real dynamic attributes related to gait, such as stride length and frequency. However, compared with sparse and unordered point cloud, image representation is regular and dense,

which facilitates the network to extract structured features for human body. Considering advantages of both modalities, we propose Geometry-Dynamic-Aware (GDA) feature fusion method by adaptively selecting valuable gait-related features from point cloud to enhance the silhouette-based features. Specifically, we leverage cross attention mechanism to make the network learn valid projection between bi-modal visual features.

We take silhouette feature as Query Q , point clouds feature as Key K and Value V for cross attention, so that the network can project significant geometry-dynamic features from point cloud to correlated image position automatically without any dependence of calibration matrices. Meanwhile, by dense queries from the image feature, we obtain fine-grained sensor-fusion features, which can benefit distinguishing individuals due to the usage of detailed local and global context.

We obtain the similarity attention map by $Q \times K$, where the higher value indicates that the queried pixel is highly correlated with the corresponding part of the point cloud feature. We select one learnt attention map queried by one position on image and visualize it in Figure 3. We can see that leg parts of the point cloud have bigger weights than the upper body, illustrating that the network really learns correspondences and pays more attention to gait-related features. Then, the attention map is further processed by a softmax normalization and used to weight point cloud features to enhance the silhouette feature:

$$F_{attention} = \text{softmax} \left(\frac{QK^T}{\sqrt{d_k}} \right) V. \quad (2)$$

The final fusion feature F_{fusion} is acquired through FFN in a transformer mechanism [49] by

$$F_{fusion} = \text{LN}(F_{attention} + \text{FFN}(F_{attention})). \quad (3)$$

4.4. Horizontal Pyramid Matching

To combine hierarchical features from the structured human body and gather both local and global informa-

tion, we use Horizontal Pyramid Mapping (HPM) [14] to split the fused silhouette feature into strips, which become a commonly-used technique in person re-identification tasks [7, 60]. The fusion feature of t th frame is split into s strip-level sets on height dimension. For each level set, the strip number is 2^{s-1} and there are $\sum_{s=1}^S 2^{s-1}$ strips in total. We denote the feature in t th frame at each strip-level set as $f'_{s,t}$. Then, temporal set pooling including MAX-pooling (MAX) and Average-pooling (AVG) is employed along temporal dimension to aggregate gait information of elements in each hierarchy of the strips.

$$f'_s = \text{MAX}(f'_{s,t}) + \text{AVG}(f'_{s,t}), \quad (4)$$

and we obtain f by combining various strips. After the classification head and feature head with multi-FC layers, $f_\alpha \in \mathcal{R}^{S \times C}$ (C denotes the number of person class) and f_β are obtained for further loss computation.

We leverage a combined loss consisting of the cross-entropy loss L_{cls} and triplet loss to train our network. L_{cls} can be computed by

$$L_{cls} = - \sum_{p=1}^S \sum_{c=1}^C g_{t_{s,c}} \log(\text{SoftMax}(f_{\alpha_s}))_c, \quad (5)$$

where $g_{t_{s,c}}$ indicates the identity information of the s th strip, which equals 0 or 1. L_{tri} is used to optimize the inter-class and intra-class distance, which is computed by

$$L_{tri} = \left[D(f_\beta^{A_i}, f_\beta^{B_k}) - D(f_\beta^{A_i}, f_\beta^{A_j}) + m \right]_+, \quad (6)$$

where A_i and A_j are samples from the same class A , while B_k denotes the sample from another class. $D(d_i, d_j)$ is the Euclidean distance between d_i and d_j and m is the margin of the triplet loss. The operation $[\gamma]_+$ equals to $\max(\gamma, 0)$.

5. Experiments

5.1. Overview

In this section, we first introduce the evaluation protocol and implementation details. Then we show extensive comparison results on the proposed LiCamGait dataset to verify the efficiency of our algorithm. Ablation studies are conducted to demonstrate the superiority of our sensor-fusion strategy. We further analyze the robustness of our method with various testing frames, changing views, and changing ranges of capture distance.

5.2. Evaluation Protocol

We select one sequence in Coat subset for every subject as the gallery data, and the remaining sequences form the probe set. Three sets of Norm, Bag, Coat are tested respectively for detailed evaluation. During the inference stage,

we assign each sample in the probe set with the label of the sample in the gallery set that is closest to it in the feature space measured by Euclidean distance. We adopt the popular Rank-k, which indicates the possibility to locate at least one true positive in top-k ranks, and mean Average Precision (mAP) as the evaluation metric. And mRank-1 represents the average Rank-1 for three subsets. For all metrics, higher values are better.

5.3. Training and Testing Details

5.3.1 Training Stage

In the training stage, we use combined loss consisting of triplet loss and cross-entropy loss. The overall loss used to train the proposed network can be formulated as

$$L = \alpha L_{tri} + \beta L_{cls}, \quad (7)$$

where α and β are the weight parameters. In our experiments, we set $\alpha = 1$ and $\beta = 0.1$. The input silhouettes are resized to 128×88 . Each LiDAR point cloud is sampled to $N = 256$ points and the sequence is normalized by translating the centroid of the first frame of point cloud to the origin of coordinates. With the Batch ALL manner, we set the batch size to (p, k) ($p = 16, k = 4$), where p denotes the number of subjects and k represents the number of training samples for each subject. In this way, when computing the triplet loss, the anchor is its own sample, the positives are the other samples with the same subject id, and the negatives are the samples of other subjects. Each of our input sequence contains 12 frames, which is close to the average length of humans' gait cycle.

5.3.2 Testing Stage

During inference, We use cosine to measure the feature similarities between the probe set and the gallery set and identify the subject by ranked similarities.

5.4. Experimental Results

5.4.1 Comparison with SOTA Methods

As shown in Table 2, we make comparison with current state-of-the-art (SOTA) gait recognition methods by using different data representations in LiCamGait, including silhouette-based GaitSet [7], GaitPart [13], GLN [17], GaitGl [30], and 2D keypoint-based GaitGraph [46], and silhouette-SMPL-based Gait3D [60]. We can see that the performances of silhouette-based methods are worse than ours mainly due to the distorted body shape in view-dependent images. Moreover, 2D keypoint-based method has the worst performance because of the inaccuracy of 2D keypoints generation from RGB images in long-range and light-varying free environment. Our performance outperforms GLN, which performs best in 2D methods, by

Table 2. Comparison with SOTA methods of gait recognition on LiCamGait. We compare our method with silhouette-based(Silh), 2D keypoint-based(2D KP), silhouette-SMPL-based(Silh&SMPL) and point cloud-based(PC) methods.

Input	Methods	NORM			BAG			COAT			mRank-1
		Rank-1	Rank-5	mAP	Rank-1	Rank-5	mAP	Rank-1	Rank-5	mAP	
Silh	GaitSet [7]	46.15	83.20	61.76	43.07	80.17	58.66	51.90	82.55	65.36	47.04
	GaitPart [13]	39.07	74.29	54.84	37.31	70.79	52.80	47.87	79.19	61.41	41.42
	GLN [17]	50.20	86.44	65.52	49.25	82.94	64.26	58.17	83.00	69.63	52.54
	GaitGL [30]	46.15	81.17	61.06	41.15	77.83	57.58	58.61	85.91	70.75	48.64
2D KP	GaitGraph [46]	15.08	42.46	29.50	17.07	40.98	30.00	21.88	39.06	32.46	18.01
Silh&SMPL	Gait3D [60]	46.36	78.93	61.40	43.27	74.95	57.61	50.98	80.91	63.90	46.87
PC	PointNet [40]	38.06	82.59	56.70	36.25	80.60	54.91	41.61	83.67	58.69	38.64
	PointMLP [32]	55.26	83.40	68.22	46.90	81.66	62.38	53.69	86.13	67.77	51.95
Silh&PC	Ours	61.44	89.61	73.31	63.67	87.70	74.30	62.39	89.57	74.10	62.50

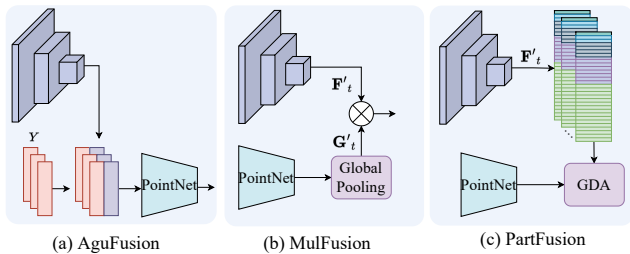


Figure 4. Different fusion methods for comparison.

11.24%, 14.42%, 4.22%, 9.96% for Rank-1 accuracy in NORM, BAG, COAT subsets and the whole dataset, respectively. Gait3D fuses the silhouettes and 3D SMPL, but these two representations are all generated from images, causing the performance also depends on the quality of images. Our method takes full advantage of the dense representation of silhouettes and geometry and dynamic information in point clouds in an effective fusion strategy, and outperforms previous method by a large margin.

5.4.2 Ablation for Modality

To demonstrate the superiority of our multi-sensor setting, we conduct ablation study for the input modalities. We have already compared with camera-only methods in above section and our method makes remarkable achievement. Considering that there are no LiDAR-only gait recognition baselines by leveraging popular point cloud feature extractor PointNet [40] and PointMLP [32] followed by a recognition head, respectively. Results are also shown in Table 2. The mRank-1 accuracy of PointMLP [32] is 51.95%, which is comparable with GLN [17], illustrating the huge potential of point clouds for gait recognition. Our LiDAR-camera-based method by effectively integrating ad-

vantages of both sensors is obviously superior to single-modal method.

5.4.3 Comparison with Fusion Methods

To further illustrate the effectiveness of our proposed GDA fusion method, we replace it with three other fusion approaches. Figure 2 shows the fusion strategies used for comparison. Comparison results are shown in Table 3. **AugFusion**, proposed by [51], expands the point cloud data with projected pixel-level feature from silhouettes. This method relies calibration matrix and establishes a hard correlation between point clouds and silhouettes, which cannot reflect the real feature relation. **MulFusion**, used by Gait3D [60], directly uses a matrix multiplication on high-level features from two modalities. Such fusion method lacks actual mapping from two modalities and overlooks the gap between the two modalities. **PartFusion** uses cross attention to fuse the point-level feature and strip-level feature at a high-dimensional level. But taking strip-level feature as query will lose a lot of fine-grained gait features, causing unsatisfactory results for gait recognition. Our GDA makes the network adaptively select valuable gait-related features from the point cloud to enhance the silhouette-based features and gain a comprehensive and fine-grained fusion-feature, which can benefit the identification.

5.4.4 More Analysis of Robustness

To verify the robustness of our method, we investigate the effect of changing views, changing capture distances, and changing numbers of testing frames.

Changing Views. To explicitly test the sensitivity to changing views, we select two sequences with totally different views as the gallery set and the probe set, respectively, for our test subjects. The experimental results are

Table 3. Comparison with different fusion methods. ‘‘Silh’’ indicates silhouette and ‘‘PC’’ means point cloud.

Input	Methods	NORM			BAG			COAT			mRank-1
		Rank-1	Rank-5	mAP	Rank-1	Rank-5	mAP	Rank-1	Rank-5	mAP	
Silh&PC	AugFusion [51]	36.24	66.44	51.27	40.00	73.46	55.28	35.53	71.93	52.27	37.26
Silh&PC	MulFusion [60]	58.50	88.06	71.22	55.44	85.29	68.86	59.91	88.37	72.50	57.95
Silh&PC	PartFusion	50.81	85.43	65.39	48.40	83.80	63.42	54.81	85.68	68.11	51.34
Silh&PC	Ours	61.44	89.61	73.31	63.67	87.70	74.30	62.39	89.57	74.10	62.50

Table 4. Experimental results for changing views.

Input	Methods	NORM	BAG	COAT	mRank-1
Silh	GLN [17]	29.03	22.58	34.38	28.66
PC	PointNet [40]	35.48	38.71	37.93	37.37
PC	PointMLP [32]	45.16	35.48	48.28	42.97
Silh&PC	Ours	51.61	48.39	65.52	55.17

Table 5. Experimental results for changing capture distances.

Distances	Methods	NORM	BAG	COAT	mRank-1
2-8m	GLN [17]	64.52	51.61	55.17	57.10
	PointNet [40]	32.26	29.03	44.83	35.37
	PointMLP [32]	51.61	38.71	55.17	48.50
	Ours	77.42	61.29	68.79	69.17
8-15m	GLN [17]	38.71	32.26	27.59	32.85
	PointNet [40]	29.03	19.35	34.38	27.59
	PointMLP [32]	35.48	29.03	44.83	36.45
	Ours	54.84	70.97	58.62	61.48

illustrated in Table 4. We can observe that the LiDAR-only methods and our multi-modal method all outperform the silhouette-only method. Because silhouette-based networks usually tend to learn appearance-related features for identification, dramatic view changes will confuse the network. LiDAR can capture view-independent depth information, which contains real gait-related features, which can help to improve the robustness to changing views.

Changing Capture Distances. The image will become low-resolution when the subject is over 10m from the sensor, which leads to low-quality silhouette results. For LiDAR, point cloud becomes sparser for farther-distance subjects. We conduct experiments at different ranges from the sensor to explore the effect of distance. We divide our test set into 2 ~ 8m and 8 ~ 15m two subsets and get results in Table 5. The performance of 2D method drops a lot with the increasing of distances due to poor segmentation results. The performances of LiDAR-only methods are more stable since even when the subject is 10m apart, the geometry and dynamic characteristics can also be recognized in point cloud. Our fusion method is the most robustness for varying

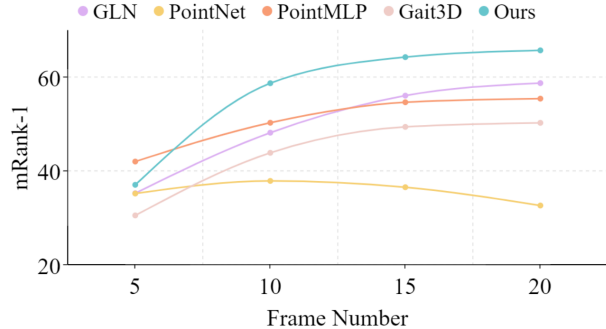


Figure 5. Average rank-1 accuracy with increasing testing frames.

distances.

Accuracy with Increasing Testing frames. We analyze the performance as the number of test frames increases. We sample 5-20 frames in each sequence of the test set and get corresponding mRank-1 accuracy values in Figure 5. Our method gets comparable results even with only one gait cycle (about 12 frames) and maintains the best performance with the number of test frames increase.

6. Future Work

Through our extensive experiments, it is surprising to see that LiDAR-only methods implemented by basic PointNet or PointMLP are comparable with 2D SOTA methods. Meanwhile, they are also robust for changing-view situations and suitable for any light conditions, indicating the potential of LiDAR for identification tasks. In the future, we will explore more effective feature extraction methods for LiDAR point cloud to further benefit gait recognition.

7. Conclusion

In this paper, we propose a new LiDAR-camera-based gait recognition solution with an effective multi-modal feature fusion strategy. We collect a new multi-modal gait recognition dataset, LiCamGait, which is collected in free scenes and provides diverse input modalities and 2D/3D representations. And our method achieves state-of-the-art performance on LiCamGait through extensive experiments. Both our novel solution and dataset can benefit and boost related research on gait recognition.

References

- [1] Jeongho Ahn, Kazuto Nakashima, Koki Yoshino, Yumi Iwashita, and Ryo Kurazume. 2v-gait: Gait recognition using 3d lidar robust to changes in walking direction and measurement distance. In *SII*, pages 602–607. IEEE, 2022. 2, 4
- [2] Inigo Alonso, Luis Riazuelo, Luis Montesano, and Ana C Murillo. 3d-mininet: Learning a 2d representation from point clouds for fast and efficient 3d lidar semantic segmentation. *RAL*, 5(4):5432–5439, 2020. 3
- [3] Weizhi An, Rijun Liao, Shiqi Yu, Yongzhen Huang, and Pong C Yuen. Improving gait recognition with 3d pose estimation. In *CCBR*, pages 137–147. Springer, 2018. 2
- [4] Weizhi An, Shiqi Yu, and etc. Performance evaluation of model-based gait on multi-view very large population database with pose sequences. *IEEE transactions on biometrics, behavior, and identity science*, 2(4):421–430, 2020. 2, 3
- [5] Xuyang Bai, Zeyu Hu, and Xinge etc. Zhu. Transfusion: Robust lidar-camera fusion for 3d object detection with transformers. In *CVPR*, pages 1090–1099, 2022. 2, 3
- [6] Csaba Benedek, Bence Gálai, Balázs Nagy, and Zsolt Jankó. Lidar-based gait analysis and activity recognition in a 4d surveillance system. *TCSVT*, 28(1):101–113, 2016. 2, 3
- [7] Hanqing Chao, Yiwei He, Junping Zhang, and Jianfeng Feng. Gaitset: Regarding gait as a set for cross-view gait recognition. In *AAAI*, volume 33, pages 8126–8133, 2019. 1, 2, 6, 7
- [8] Qi Chen, Lin Sun, Zhixin Wang, Kui Jia, and Alan Yuille. Object as hotspots: An anchor-free 3d object detection approach via firing of hotspots. In *ECCV*, pages 68–84. Springer, 2020. 3
- [9] Xiaozhi Chen, Huimin Ma, Ji Wan, Bo Li, and Tian Xia. Multi-view 3d object detection network for autonomous driving. pages 6526–6534, 2017. 3
- [10] Peishan Cong, Xinge Zhu, Feng Qiao, Yiming Ren, Xidong Peng, Yuenan Hou, Lan Xu, Ruiqiang Yang, Dinesh Manocha, and Yuexin Ma. Stcrowd: A multimodal dataset for pedestrian perception in crowded scenes. In *CVPR*, pages 19608–19617, 2022. 1, 3
- [11] Yudi Dai, Yi Lin, Chenglu Wen, Siqi Shen, Lan Xu, Jingyi Yu, Yuexin Ma, and Cheng Wang. Hsc4d: Human-centered 4d scene capture in large-scale indoor-outdoor space using wearable imus and lidar. *CVPR*, pages 6782–6792, 2022. 1, 3
- [12] K DAVID WAGG. On automated model-based extraction and analysis of gait. *Automatic Face and Gesture Recognition, Proceedings. Sixth IEEE international Conference, 2004*, 2004. 2
- [13] Chao Fan, Yunjie Peng, and Chunshui etc. Cao. Gaitpart: Temporal part-based model for gait recognition. In *CVPR*, pages 14225–14233, 2020. 1, 2, 6, 7
- [14] Yang Fu, Yunchao Wei, and etc. Zhou. Horizontal pyramid matching for person re-identification. In *AAAI*, volume 33, pages 8295–8302, 2019. 6
- [15] Fangzhou Hong, Hui Zhou, Xinge Zhu, Hongsheng Li, and Ziwei Liu. Lidar-based panoptic segmentation via dynamic shifting network. *CVPR*, pages 13085–13094, 2021. 4
- [16] Md Altam Hossain, Yasushi Makihara, Junqiu Wang, and Yasushi Yagi. Clothing-invariant gait identification using part-based clothing categorization and adaptive weight control. *PR*, 43(6):2281–2291, 2010. 2
- [17] Saihui Hou, Chunshui Cao, Xu Liu, and Yongzhen Huang. Gait lateral network: Learning discriminative and compact representations for gait recognition. In *ECCV*, pages 382–398. Springer, 2020. 1, 2, 6, 7, 8
- [18] Yuenan Hou, Xinge Zhu, Yuexin Ma, Chen Change Loy, and Yikang Li. Point-to-voxel knowledge distillation for lidar semantic segmentation. *2022 IEEE/CVF Conference on Computer Vision and Pattern Recognition (CVPR)*, pages 8469–8478, 2022. 1
- [19] Xiaohu Huang, Duowang Zhu, and Hao etc. Wang. Context-sensitive temporal feature learning for gait recognition. In *ICCV*, pages 12909–12918, 2021. 2
- [20] Haruyuki Iwama, Mayu Okumura, Yasushi Makihara, and Yasushi Yagi. The ou-isir gait database comprising the large population dataset and performance evaluation of gait recognition. *TIFS*, 7(5):1511–1521, 2012. 2, 3, 4
- [21] Kooksung Jun, Deok-Won Lee, Kyoobin Lee, Sanghyub Lee, and Mun Sang Kim. Feature extraction using an rnn autoencoder for skeleton-based abnormal gait recognition. *IEEE Access*, 8:19196–19207, 2020. 2
- [22] Jason Ku, Melissa Mozifian, Jungwook Lee, Ali Harakeh, and Steven L Waslander. Joint 3d proposal generation and object detection from view aggregation. In *IROS*, pages 1–8. IEEE, 2018. 3
- [23] Munish Kumar, Navdeep Singh, Ravinder Kumar, Shubham Goel, and Krishan Kumar. Gait recognition based on vision systems: A systematic survey. *J. Vis. Commun. Image Represent.*, 75:103052, 2021. 1, 2
- [24] Jialian Li and etc. Lidarcap: Long-range marker-less 3d human motion capture with lidar point clouds. In *CVPR*, pages 20502–20512, 2022. 1, 3
- [25] Xiang Li, Yasushi Makihara, Chi Xu, and Yasushi Yagi. End-to-end model-based gait recognition using synchronized multi-view pose constraint. In *ICCV*, pages 4106–4115, 2021. 2
- [26] Yingwei Li, Adams Wei Yu, and etc. Meng. Deepfusion: Lidar-camera deep fusion for multi-modal 3d object detection. In *CVPR*, pages 17182–17191, 2022. 3
- [27] Ming Liang, Bin Yang, Shenlong Wang, and Raquel Urtasun. Deep continuous fusion for multi-sensor 3d object detection. In *ECCV*, pages 641–656, 2018. 3
- [28] Tingting Liang, Hongwei Xie, and etc. Yu. Bevfusion: A simple and robust lidar-camera fusion framework. *arXiv preprint arXiv:2205.13790*, 2022. 2, 3
- [29] Rijun Liao, Shiqi Yu, Weizhi An, and Yongzhen Huang. A model-based gait recognition method with body pose and human prior knowledge. *PR*, 98:107069, 2020. 2
- [30] Beibei Lin, Shunli Zhang, and Xin Yu. Gait recognition via effective global-local feature representation and local temporal aggregation. In *ICCV*, pages 14648–14656, 2021. 1, 2, 6, 7

- [31] Matthew Loper, Naureen Mahmood, Javier Romero, Gerard Pons-Moll, and Michael J. Black. Smpl: a skinned multi-person linear model. *ACM Trans. Graph.*, 34:248:1–248:16, 2015. [2](#)
- [32] Xu Ma, Can Qin, Haoxuan You, Haoxi Ran, and Yun Fu. Rethinking network design and local geometry in point cloud: A simple residual mlp framework. *arXiv preprint arXiv:2202.07123*, 2022. [7](#), [8](#)
- [33] Yasushi Makihara. Silhouette transformation based on walking speed for gait identification. In *CVPR*, 2010. [2](#), [3](#)
- [34] Yasushi Makihara, Hidetoshi Mannami, and Yasushi Yagi. Gait analysis of gender and age using a large-scale multi-view gait database. In *ACCV*, pages 440–451. Springer, 2010. [2](#)
- [35] Andres Milioto, Ignacio Vizzo, Jens Behley, and Cyrill Stachniss. Rangenet++: Fast and accurate lidar semantic segmentation. In *IROS*, pages 4213–4220. IEEE, 2019. [3](#)
- [36] Sourabh A. Niyogi and Edward H. Adelson. Analyzing and recognizing walking figures in xyt. *CVPR*, pages 469–474, 1994. [1](#)
- [37] Yunjie Peng, Saihui Hou, Kang Ma, Yang Zhang, Yongzhen Huang, and Zhiqiang He. Learning rich features for gait recognition by integrating skeletons and silhouettes. *arXiv preprint arXiv:2110.13408*, 2021. [1](#), [2](#)
- [38] AJ Piergiovanni, Vincent Casser, Michael S Ryoo, and Anelia Angelova. 4d-net for learned multi-modal alignment. In *ICCV*, pages 15435–15445, 2021. [3](#)
- [39] Charles R Qi, Xinlei Chen, and etc. Imvotenet: Boosting 3d object detection in point clouds with image votes. In *CVPR*, pages 4404–4413, 2020. [3](#)
- [40] Charles R Qi, Hao Su, Kaichun Mo, and Leonidas J Guibas. Pointnet: Deep learning on point sets for 3d classification and segmentation. In *CVPR*, pages 652–660, 2017. [5](#), [7](#), [8](#)
- [41] Sudeep Sarkar, P Jonathon Phillips, Zongyi Liu, Isidro Robledo Vega, Patrick Grother, and Kevin W Bowyer. The humanid gait challenge problem: Data sets, performance, and analysis. *TPAMI*, 27(2):162–177, 2005. [3](#)
- [42] Shaoshuai Shi, Zhe Wang, Jianping Shi, Xiaogang Wang, and Hongsheng Li. From points to parts: 3d object detection from point cloud with part-aware and part-aggregation network. *TPAMI*, 43(8):2647–2664, 2020. [3](#)
- [43] Yu Sun, Qian Bao, Wu Liu, Yili Fu, Michael J Black, and Tao Mei. Monocular, one-stage, regression of multiple 3d people. In *ICCV*, pages 11179–11188, 2021. [3](#), [4](#)
- [44] Noriko Takemura and Yasushi etc. Makihara. Multi-view large population gait dataset and its performance evaluation for cross-view gait recognition. *IPSJ Transactions on Computer Vision and Applications*, 10(1):1–14, 2018. [3](#)
- [45] Daoliang Tan, Kaiqi Huang, Shiqi Yu, and Tieniu Tan. Efficient night gait recognition based on template matching. In *ICPR*, volume 3, pages 1000–1003. IEEE, 2006. [2](#), [3](#)
- [46] Torben Teepe, Ali Khan, Johannes Gilg, Fabian Herzog, Stefan Hörmann, and Gerhard Rigoll. Gaitgraph: Graph convolutional network for skeleton-based gait recognition. In *ICIP*, pages 2314–2318. IEEE, 2021. [1](#), [2](#), [6](#), [7](#)
- [47] Rahul Thour and Prof. (Dr.) R. K. Bathla. Gait recognition system: A survey. *Journal of University of Shanghai for Science and Technology*, 2021. [1](#), [2](#)
- [48] Md Uddin and Thanh Trung etc. Ngo. The ou-isir large population gait database with real-life carried object and its performance evaluation. *IPSJ Transactions on Computer Vision and Applications*, 10(1):1–11, 2018. [2](#)
- [49] Ashish Vaswani, Noam M. Shazeer, Niki Parmar, Jakob Uszkoreit, Llion Jones, Aidan N. Gomez, Lukasz Kaiser, and Illia Polosukhin. Attention is all you need. *ArXiv*, abs/1706.03762, 2017. [5](#)
- [50] Sourabh Vora, Alex H Lang, Bassam Helou, and Oscar Beijbom. Pointpainting: Sequential fusion for 3d object detection. In *CVPR*, pages 4604–4612, 2020. [2](#), [3](#)
- [51] Chunwei Wang, Chao Ma, Ming Zhu, and Xiaokang Yang. Pointaugmenting: Cross-modal augmentation for 3d object detection. In *CVPR*, pages 11794–11803, 2021. [2](#), [3](#), [7](#), [8](#)
- [52] Jingdong Wang and Ke etc. Sun. Deep high-resolution representation learning for visual recognition. *TPAMI*, 43(10):3349–3364, 2020. [4](#)
- [53] Liang Wang, Tieniu Tan, Huazhong Ning, and Weiming Hu. Silhouette analysis-based gait recognition for human identification. *TPAMI*, 25(12):1505–1518, 2003. [2](#), [3](#)
- [54] Yuan Wang, Tianyue Shi, Peng Yun, Lei Tai, and Ming Liu. Pointseg: Real-time semantic segmentation based on 3d lidar point cloud. *arXiv preprint arXiv:1807.06288*, 2018. [3](#)
- [55] ChewYean Yam, Mark S Nixon, and John N Carter. Automated person recognition by walking and running via model-based approaches. *PR*, 37(5):1057–1072, 2004. [2](#)
- [56] Bin Yang, Wenjie Luo, and Raquel Urtasun. Pixor: Real-time 3d object detection from point clouds. In *CVPR*, pages 7652–7660, 2018. [3](#)
- [57] Shiqi Yu, Daoliang Tan, and Tieniu Tan. A framework for evaluating the effect of view angle, clothing and carrying condition on gait recognition. In *ICPR*, volume 4, pages 441–444. IEEE, 2006. [2](#), [3](#), [4](#)
- [58] Yang Zhang and etc. Polarnet: An improved grid representation for online lidar point clouds semantic segmentation. In *CVPR*, pages 9601–9610, 2020. [3](#)
- [59] Chengfeng Zhao, Yiming Ren, Yannan He, Peishan Cong, Han Liang, Jingyi Yu, Lan Xu, and Yuexin Ma. Lidar-aid inertial poser: Large-scale human motion capture by sparse inertial and lidar sensors. *arXiv preprint arXiv:2205.15410*, 2022. [1](#), [3](#)
- [60] Jinkai Zheng, Xinchun Liu, Wu Liu, Lingxiao He, Chenggang Yan, and Tao Mei. Gait recognition in the wild with dense 3d representations and a benchmark. In *CVPR*, pages 20228–20237, 2022. [1](#), [2](#), [3](#), [4](#), [6](#), [7](#), [8](#)
- [61] Xinge Zhu, Yuexin Ma, Tai Wang, Yan Xu, Jianping Shi, and Dahua Lin. Ssn: Shape signature networks for multi-class object detection from point clouds. In *ECCV*, pages 581–597. Springer, 2020. [3](#)
- [62] Xinge Zhu, Hui Zhou, Tai Wang, Fangzhou Hong, Yuexin Ma, Wei Li, Hongsheng Li, and Dahua Lin. Cylindrical and asymmetrical 3d convolution networks for lidar segmentation. *CVPR*, pages 9934–9943, 2021. [1](#), [3](#)
- [63] Zheng Zhu, Xianda Guo, and Tian etc. Yang. Gait recognition in the wild: A benchmark. In *ICCV*, pages 14789–14799, 2021. [2](#), [3](#), [4](#)